String-Stable CACC Design and Experimental Validation: A Frequency-Domain Approach

Gerrit J. L. Naus, René P. A. Vugts, Jeroen Ploeg, Marinus (René) J. G. van de Molengraft, and Maarten Steinbuch, *Senior Member, IEEE*

***Abstract*—The design of a cooperative adaptive cruise-control (CACC) system and its practical validation are presented. Focusing on the feasibility of implementation, a decentralized controller design with a limited communication structure is proposed (in this case, a wireless communication link with the nearest preceding vehicle only). A necessary and sufficient frequency-domain condition for string stability is derived, taking into account heterogeneous traffic, i.e., vehicles with possibly different characteristics. For a velocity-dependent intervehicle spacing policy, it is shown that the wireless communication link enables driving at small intervehicle distances, whereas string stability is guaranteed. For a constant velocity-independent intervehicle spacing, string stability cannot be guaranteed. To validate the theoretical results, experiments are performed with two CACC-equipped vehicles. Implementation of the CACC system, the string-stability characteristics of the practical setup, and experimental results are discussed, indicating the advantages of the design over standard adaptive-cruise-control functionality.**

***Index Terms*—Cooperative adaptive cruise control (CACC), cooperative systems, road vehicles, string stability.**

I. Introduction

COOPERATIVE adaptive cruise control (CACC) is an extension of the adaptive cruise control (ACC) functionality. Nowadays, the ACC functionality is widespread and available in numerous commercially available vehicles. ACC automatically adapts the cruise-control velocity of a vehicle if there is preceding traffic that drives very close and at a lower velocity. Commonly, radar is adopted to detect preceding traffic. Because ACC is primarily intended as a comfort system and, to a smaller degree, as a safety system, relatively large intervehicle distances are adopted in commercially available systems [1]–[3]. Decreasing the intervehicle distance to a small value of only a few meters is expected to yield an increase in traffic throughput. Moreover, specifically focusing on heavy-duty vehicles, a significant reduction in the aerodynamic drag force is possible, thus decreasing fuel consumption [4], [5]. Consequently, it is desirable to enable this design for larger strings of vehicles, i.e., the so-called platoons.

When the commercially available ACC functionality is employed to achieve such small intervehicle distances, string-unstable driving behavior may result. The string stability of a platoon indicates whether oscillations are amplified upstream the traffic flow [6]. The longitudinal dynamics of the platoon are called string stable if sudden changes in the velocity of a vehicle at the front of a platoon are attenuated by the vehicles upstream the platoon. If changes in the velocity of a vehicle at the front of a platoon are amplified by the vehicles upstream the platoon, the longitudinal dynamics of the platoon are called string unstable. One example of string-unstable behavior is the forming of traffic jams that occur for no apparent reason. No accident or bottleneck needs to be present, and only too much traffic or erratic driving behavior may cause a shockwave of continuously increased braking upstream a string of vehicles, until vehicles come to a halt, and a traffic jam results [7]. Consequently, considering traffic throughput and fuel economy, as well as comfort and safety, string-unstable driving behavior is highly undesirable.

Extending the standard ACC functionality with a wireless intervehicle communication link enables driving at small intervehicle distances while maintaining string stability [8]. The resulting functionality is called CACC. The design of the CACC functionality has extensively been discussed in the literature (e.g., see [2], [5], and [8]–[11]). However, a generic approach for the design of a CACC system does not (yet) exist. In most cases, a specific system setup and corresponding working conditions are considered, rather than true generalizations. Furthermore, the focus is often on theoretical analysis of the system, rather than on the possibilities for practical implementation. In this paper, a CACC design that specifically focuses on the feasibility of implementation is proposed.

The contribution of this paper involves, first, the design of a CACC system that focuses on the feasibility of implementation and the definition of a corresponding sufficient frequency-domain condition for the string stability of heterogeneous traffic. Second, a theoretical analysis and, in particular, experimental validation of the proposed CACC system are presented. The results are an extension of our work published in [12].

In Sections II and III, the problem formulation and the CACC design are presented. The definition of string stability and the string-stability characteristics of the system are discussed in Sections IV and V. In Section VI, experimental validation is presented using two Citroën C4s. This paper is closed with conclusions and an outlook on future work.

Manuscript received January 22, 2010; revised June 14, 2010; accepted August 4, 2010. Date of publication September 13, 2010; date of current version November 12, 2010. The review of this paper was coordinated by Dr. K. Deng.

G. J. L. Naus, R. P. A. Vugts, M. (R.) J. G. van de Molengraft, and M. Steinbuch are with the Control Systems Technology Group, Department of Mechanical Engineering, Eindhoven University of Technology, 5600 MB Eindhoven, The Netherlands (e-mail: g.j.l.naus@tue.nl; r.p.a.vugts@tue.nl; m.j.g.v.d.molengraft@tue.nl; m.steinbuch@tue.nl).

J. Ploeg is with the Automotive Business Unit, Netherlands Organization for Applied Scientific Research, 5700 AT Helmond, The Netherlands (e-mail: j.ploeg@tno.nl).

Color versions of one or more of the figures in this paper are available online at http://ieeexplore.ieee.org.

Digital Object Identifier 10.1109/TVT.2010.2076320

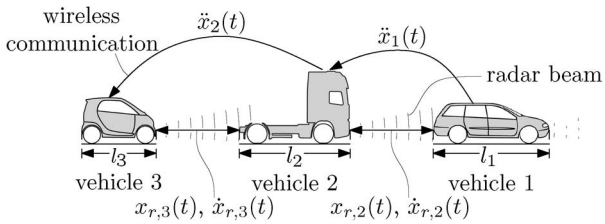

Fig. 1. Schematic of a platoon of vehicles equipped with the CACC functionality, where $x_{r,i}(t)$, $\dot{x}_{r,i}(t)$, $\ddot{x}_i(t)$, and l_i represent the relative position, the relative velocity, the acceleration, and the length of vehicle i, respectively.

II. Problem Formulation

A. CACC System Setup

In Fig. 1, a schematic of a platoon of vehicles equipped with the CACC functionality is shown, where $x_{r,i}(t)$, $\dot{x}_{r,i}(t)$, $\ddot{x}_i(t)$, and l_i are the relative position, the relative velocity, the acceleration, and the length of vehicle i, respectively.

Focusing on the feasibility of implementation, a decentralized controller design is pursued, as opposed to a centralized design [13]. Communication with the nearest preceding vehicle is adopted, as schematically depicted in Fig. 1. Examples of other communication structures include a centralized controller design and communication between all vehicles in a platoon [13], bidirectional communication with the nearest vehicles [6], [14], or communication with both the nearest vehicles and a designated platoon leader [8], [15]. Communication with the directly preceding vehicle only is often called semiautonomous ACC and facilitates easy implementation.

Similar to the communication structure, the variety in spacing policies that are proposed in the literature, i.e., the desired distance between the vehicles in a platoon, is large [16], [17]. For example, a constant spacing policy [8], a velocity-dependent spacing policy [18], or more complex nonlinear spacing policies [14] are considered. Focusing on the feasibility of implementation rather than on the definition of a new spacing policy, the most common policy is adopted, including a constant part and a velocity-dependent part [8], [18].

The CACC design is based on a standard ACC system. Moreover, the additional data that are available through the wireless communication link is used in a feedforward setting. Hence, the ACC functionality is still available if no communication is present [8], [19]. Furthermore, heterogeneous traffic is considered, i.e., a platoon of vehicles with possibly different characteristics, as is the case in actual traffic. In the literature, however, homogeneous traffic is often considered instead, i.e., vehicles with identical characteristics (e.g., [20] and [21]). Finally, delay in the communication signal is taken into account. The effect of delay in the communicated data is often neglected (e.g., see [8] and [18]), with some notable exceptions, as shown in [9], [10], and [22].

B. String Stability

Considering the definition of the string stability of a platoon of vehicles, much ambiguity is present in the literature. The common part in the definitions is that they all consider amplification of oscillations upstream a string of vehicles, i.e., from vehicle $i = 1$ to vehicle $i > 1$ (see Fig. 1) [6]. However, oscillations in different signals are considered.

Focusing on preventing collisions, the errors $e_i(t)$ between the desired and the actual intervehicle distances are often considered. Correspondingly, the driving behavior of a platoon is denoted string stable if these errors do not amplify upstream a platoon [14], [15], [17], [23]–[26]. A modification on this definition is presented in [27], considering the amplification of oscillations in the intervehicle distances $x_{r,i}(t)$.

For the case of heterogeneous traffic, the amplification of oscillations in the absolute vehicle positions $x_i(t)$ or in the vehicle velocities $\dot{x}_i(t)$ is considered in [6], [21], [28], and [29]. In these papers, the focus is on oscillations, as discussed in the Introduction, which, for example, result in traffic jams. Finally, in some cases, the error signals are considered for analysis, whereas the absolute vehicle positions and velocities are considered when evaluating the results [2], [8], [11], [16].

Furthermore, both time- and frequency-domain conditions are presented, e.g., [9] and [29]. In this paper, a frequency-domain approach is adopted. The definition of string stability is revised, focusing on the feasibility of implementation, i.e., for a decentralized controller design, communication with the directly preceding vehicle only and heterogeneous traffic. This approach yields a necessary and sufficient definition for string stability. Adopting a linear frequency-domain approach enables easy and intuitive analysis, focusing on the amplification of oscillations. The resulting condition for string stability is used to compare the characteristics of the standard ACC functionality and the proposed CACC system, indicating the benefits of the wireless communication link.

III. Control Structure

The CACC design is based on a standard ACC system and the most commonly used spacing policy. In this section, the ACC design, the spacing policy, and the CACC design are discussed.

A. ACC Control Structure

Consider a string of heterogeneous vehicles, as depicted in Fig. 1, where $x_{r,i}(t)$, $\dot{x}_{r,i}(t)$, $\ddot{x}_i(t)$, and l_i are the relative position, the relative velocity, the acceleration, and the length of vehicle i, respectively. The primary control objective for each vehicle is to follow the corresponding preceding vehicle at a desired distance, i.e., a desired relative position $x_{r,d,i}(t)$. Using radar, the relative position $x_{r,i}(t) = x_{i-1}(t) - x_i(t)$ and the corresponding relative velocity $\dot{x}_{r,i}(t)$ are measured, where the vehicle length l_i is not taken into account (see Fig. 1).

In a standard ACC system, the radar output data are used in a feedback setting. A feedback controller controls the spacing error $e_i(t) = x_{r,i}(t) - x_{r,d,i}(t)$ between the desired distance and the actual distance. Defining $e_i(t)$ in this manner implies that a positive control action, i.e., acceleration, is required when the intervehicle distance $x_{r,i}(t)$ is very large with respect to the desired distance $x_{r,d,i}(t)$. This condition makes the control action, which is defined as $u_i(t)$, intuitive. The resulting control setup is schematically depicted in Fig. 2. For analysis, the radar output data are reconstructed based on the positions of the

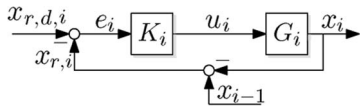

Fig. 2. ACC control structure, where $G_i = G_i(s)$ represent the dynamics of the ith vehicle, and $K_i = K_i(s)$ is the corresponding ACC feedback controller, for $i \geq 1$. For clarity, the time dependency of the signals is omitted.

vehicles i and $i-1$. The models $G_i(s)$ and $K_i(s)$ represent linear transfer function models, where s is the Laplace operator. For clarity, this dependency is omitted in the figures.

It is assumed that the model $G_i(s)$ includes a (low-level) control loop for the longitudinal vehicle dynamics. Consequently, the input $u_i(t)$ of $G_i(s)$ can be regarded as a desired acceleration $\ddot{x}_{d,i}(t)$. The low-level control loop ensures tracking of this desired acceleration through the actuation of the throttle and the brake system. It is assumed that the low-level closed-loop longitudinal vehicle dynamics of vehicle i can be represented by

$$G_i(s) = \frac{k_{G,i}}{s^2(\tau_i s + 1)} e^{-\phi_i s}, \qquad \text{for } i \geq 1 \tag{1}$$

where $\tau_i^{-1} = \omega_{bw,l,i}$ is the low-level closed-loop bandwidth, $k_{G,i}$ is the model gain, which, ideally, is equal to 1, and ϕ_i represents the actuator and internal communication delay time.

Consider the closed-loop complementary sensitivity transfer function

$$T_i'(s) = \frac{G_i(s)K_i(s)}{1 + G_i(s)K_i(s)}, \qquad \text{for } i \geq 1. \tag{2}$$

Define the bandwidth $\omega_{bw,i}'$ of $T_i'(s)$ as the frequency at which the magnitude of the open-loop frequency response function $L_i'(j\omega) = G_i(j\omega)K_i(j\omega)$ crosses 0 dB in the downward sense. Given the vehicle dynamics $G_i(s)$ (1) with reasonably small ϕ_i, a standard proportional–derivative (PD) controller provides the freedom to choose a desired bandwidth $\omega_{bw,i}'$, with a desired phase margin $\alpha_{PM,i}'$. Correspondingly, the ACC feedback controller $K_i(s)$ that is considered in this paper is given by

$$K_i(s) = k_{P,i} + k_{D,i}s, \qquad \text{for } i \geq 1. \tag{3}$$

The values for $k_{P,i}$ and $k_{D,i}$ can straightforwardly be computed using $|L_i'(j\omega_{bw,i}')| = 1$ and $\angle L_i'(j\omega_{bw,i}') = \alpha_{PM,i}'$. In this paper, $k_{P,i} = k_{D,i}^2 = \omega_{K,i}^2$ is used, which yields

$$K_i(s) = \omega_{K,i}(\omega_{K,i} + s), \qquad \text{for } i \geq 1. \tag{4}$$

B. Spacing Policy

The desired relative position or distance $x_{r,d,i}(t)$ is determined by the so-called spacing policy. The most common policy includes a constant part [8] and, optionally, a velocity-dependent part [18], which is given by

$$x_{r,d,i}(t) = x_{r,0,i} + h_{d,i}\dot{x}_i(t), \qquad \text{for } i \geq 1 \tag{5}$$

where $x_{r,0,i}$ is the constant part or the desired distance at standstill, $h_{d,i}$ is the so-called desired headway time, and $\dot{x}_i(t)$ is the velocity of vehicle i, for $i \geq 1$. Hence, the headway time $h_{d,i}$ represents the time that it takes for vehicle i to bridge the distance in between the vehicles i and $i-1$ when continuing to drive with a constant velocity.

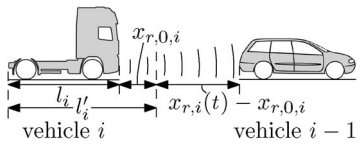

Fig. 3. Schematic of two vehicles driving in a platoon, where l_i is the actual vehicle length of vehicle i, $x_{r,0,i}$ is the desired distance at standstill, $x_{r,i}(t)$ is the relative position, and $l_i' = l_i + x_{r,0,i}$ is the vehicle length considered for analysis.

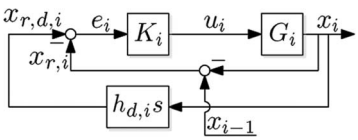

Fig. 4. ACC control structure, where $G_i = G_i(s)$ represent the dynamics of the ith vehicle, $K_i = K_i(s)$ is the corresponding ACC feedback controller, s is the Laplace operator, and $h_{d,i}$ is the headway time. For clarity, the time dependency of the signals is omitted.

The desired distance at standstill $x_{r,0,i}$ can be regarded as an extension of the vehicle length l_i, i.e., $l_i' = l_i + x_{r,0,i}$, as schematically depicted in Fig. 3. Hence, the desired distance at standstill is not considered in the rest of this paper. This yields

$$x_{r,d,i}(t) = h_{d,i}\dot{x}_i(t), \qquad \text{for } i \geq 1. \tag{6}$$

Correspondingly, the relative position of the vehicles is redefined, with slight abuse of notation, by

$$x_{r,i}(t) \triangleq x_{r,i}(t) - x_{r,0,i}. \tag{7}$$

For $h_{d,i} = 0.0$ s, a constant spacing policy results. For $h_{d,i} > 0.0$ s, the spacing policy (6) is called a constant headway time policy, targeting a constant intervehicle time gap of $h_{d,i}$ s. In the system analysis further on, both the constant spacing policy and the constant headway time policy are considered.

As a result of the velocity-dependent spacing policy, the control structure becomes cascaded, as schematically depicted in Fig. 4. The design of the outer loop of the cascaded controller comes down to the choice for the headway time $h_{d,i}$. The corresponding closed-loop transfer $T_i(s)$ equals

$$T_i(s) = \frac{G_i(s)K_i(s)}{1 + H_i(s)G_i(s)K_i(s)}, \qquad \text{for } i \geq 1 \tag{8}$$

where

$$H_i(s) = 1 + h_{d,i}s, \qquad \text{for } i \geq 1 \tag{9}$$

includes the spacing-policy dynamics (6). The stability of the closed-loop system $T_i(s)$ is positively affected by $h_{d,i} \geq 0$, which follows from the comparison of $L_i(s)$ and $L_i'(s)$.

C. CACC Control Structure

As discussed in the Introduction, wireless communication with the nearest preceding vehicle is considered for the CACC system. Through this communication channel, the acceleration

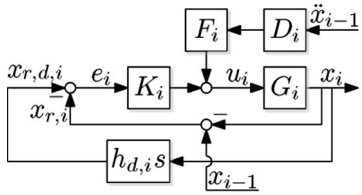

Fig. 5. CACC control structure, where $G_i = G_i(s)$ represent the dynamics of the ith vehicle, $K_i = K_i(s)$ is the corresponding ACC feedback controller, $F_i = F_i(s)$ is the feedforward filter, $D_i = D_i(s)$ is the communication delay, s is the Laplace operator, and $h_{d,i}$ the headway time. For clarity, the time dependency of the signals is omitted.

of the preceding vehicle $\ddot{x}_{i-1}(t)$ is available (see Fig. 1). The wirelessly communicated data are used in a feedforward setting, extending the standard ACC feedback controller to the CACC functionality. As a result, the system can degrade to a standard ACC system when no communication is present or if communication fails.

The acceleration of the preceding vehicle is used as a feedforward control signal through a feedforward filter $F_i(s)$. The acceleration is obtained through wireless communication, which includes a communication delay $D_i(s)$. The resulting control structure is schematically depicted in Fig. 5.

The delay is represented by a constant delay time θ_i, yielding

$$\mathcal{L}\left(\ddot{x}_{i-1}(t-\theta_i)\right) = D_i(s)s^2 X_{i-1}(s) \tag{10}$$

where

$$D_i(s) = e^{-\theta_i s}, \qquad \text{for } i > 1 \tag{11}$$

and $\mathcal{L}(\cdot)$ denotes the Laplace transformation. The design of the feedforward filter is based on a zero-error condition, where the Laplace transform of the error $e_i(t)$ is defined as

$$\mathcal{L}\left(e_i(t)\right) = \frac{1 - H_i(s)G_i(s)F_i(s)D_i(s)s^2}{1 + H_i(s)G_i(s)K_i(s)}\mathcal{L}\left(x_{i-1}(t)\right), \text{ for } i > 1. \tag{12}$$

Considering $\mathcal{L}(e_i(t))$ (12), the communication delay $D_i(s)$ can only be compensated for using an estimator for the communicated acceleration signal. In this paper, it is assumed that such an estimator is not available. However, in the subsequent system analysis, both a system with and a system without communication delay are considered. The latter system is representative of the case that an appropriately designed estimator is available. Hence, demanding $\mathcal{L}(e_i(t)) = 0$, taking into account a communication delay $D_i(s)$ in (11) that is not compensated for by the feedforward filter, yields

$$F_i(s) = \left(H_i(s)G_i(s)s^2\right)^{-1}, \qquad \text{for } i > 1. \tag{13}$$

IV. String Stability: A Frequency-Domain Approach

In this section, the definition of string stability is revised, following a frequency-domain approach (see Section II). The focus is on the feasibility of application in practice. Hence, heterogeneous traffic is considered, a decentralized controller design is pursued, and communication with the directly preceding vehicle only is considered. It is shown that, in that case, the frequency-domain system state $X_i(s)$ has to be considered to define the string stability of a platoon of vehicles, which is directly related to the absolute vehicle positions $x_i(t)$ or the vehicle velocities $\dot{x}_i(t)$.

Consider the CACC control structure shown in Fig. 5. Coupling several of these control structures yields the control structure for a platoon of vehicles, as shown in Fig. 6, where the inner and the outer control loops (see Fig. 5) are merged using the definition of $H_i(s)$ (9). The first vehicle in the platoon, $i = 1$, is assumed to follow a given time-varying reference position $x_0(t)$ using radar measurements. The other vehicles, i.e., $i > 1$, use both the radar and the wireless communication.

Define the Laplace transforms of the input $\mathcal{L}(x_0(t)) = X_0(s)$ and the signals $u_i(t)$, $x_i(t)$, and $e_i(t)$, i.e., $\mathcal{L}(u_i(t)) = U_i(s)$, $\mathcal{L}(x_i(t)) = X_i(s)$, and $\mathcal{L}(e_i(t)) = E_i(s)$. Next, define the so-called string-stability transfer functions $\mathcal{G}'_{\Lambda,i'}(s)$, $\Lambda \in \{U, X, E\}$. We have

$$\mathcal{G}'_{\Lambda,i'}(s) = \frac{\Lambda_{i'}(s)}{\Lambda_1(s)} = \frac{\Lambda_{i'}(s)}{X_0(s)}\left(\frac{\Lambda_1(s)}{X_0(s)}\right)^{-1}, \quad \text{for } i' > 1 \tag{14}$$

where i' denotes the last vehicle in a platoon of vehicles. The magnitude of the string-stability transfer functions $\mathcal{G}'_{\Lambda,i'}(s)$ is a measure for the amplification of oscillations upstream a platoon. Hence, because string stability is defined as the damping of the magnitude of oscillations upstream from a platoon, a necessary condition for string stability is (e.g., see [15] and [30])

$$\left\|\mathcal{G}'_{\Lambda,i'}(j\omega)\right\|_\infty \leq 1, \qquad \text{for } i' > 1 \tag{15}$$

in which $\|\cdot\|_\infty$ denotes the maximum amplitude for all ω. In the case that

$$\left\|\mathcal{G}'_{\Lambda,i'}(j\omega)\right\|_\infty = 1, \qquad \text{for } i' > 1,\ \omega > 0 \tag{16}$$

holds, this condition is called the marginal string stability.

Targeting a decentralized controller design, the dynamics of all vehicles $k \in \{1, \ldots, i'-1\}$ have to be known to fulfill (15). For heterogeneous traffic, i.e., vehicles with possibly different characteristics and dynamics, this condition requires an extensive communication structure. Because communication with the nearest preceding vehicle only is considered, more conservative string-stability transfer functions $\mathcal{G}_{\Lambda,i}(s)$, $\Lambda \in \{U, X, E\}$ are defined as follows:

$$\mathcal{G}_{\Lambda,i}(s) = \frac{\Lambda_i(s)}{\Lambda_{i-1}(s)} = \frac{\Lambda_i(s)}{X_0(s)}\left(\frac{\Lambda_{i-1}(s)}{X_0(s)}\right)^{-1}, \quad \text{for } i > 1 \tag{17}$$

which yields a more conservative sufficient condition for string stability, i.e.,

$$\left\|\mathcal{G}_{\Lambda,i}(j\omega)\right\|_\infty \leq 1, \qquad \text{for } i > 1. \tag{18}$$

Analogously, a sufficient condition for the marginal string stability is $\|\mathcal{G}_{\Lambda,i}(j\omega)\|_\infty = 1$, for $i > 1$, $\omega > 0$. Because it holds that

$$\mathcal{G}'_{\Lambda,i}(s) = \prod_{k=2}^{i} SS_{\Lambda,k}(s), \qquad \text{for } i > 1 \tag{19}$$

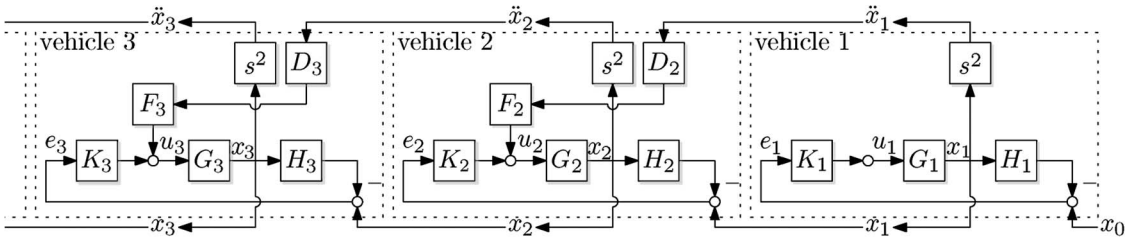

Fig. 6. Control structure of a platoon of vehicles, where $G_i = G_i(s)$ represent the dynamics of the ith vehicle, $K_i = K_i(s)$ is the corresponding ACC feedback controller, $F_i = F_i(s)$ is the feedforward controller, $D_i = D_i(s)$ is the communication delay, and $H_i = H_i(s)$ represents the spacing policy dynamics, for $i \in \{1, 2, 3\}$. For clarity, the time dependency of the signals is omitted.

TABLE I
SYSTEM PARAMETERS FOR A STRING OF HETEROGENEOUS VEHICLES

i vehicle	$k_{G,i}$ [-]	τ_i [s/rad]	ϕ_i [s]	$\omega_{K,i}$ [rad/s]	θ_i [s]	ε_i [-]	$h_{d,i}$ [s]
1	0.7	0.1	0.0	3.0	0.1	1.0	1.0
2	1.0	0.5	0.1	0.3	0.3	0.8	1.0
3	1.3	0.4	0.3	1.0	0.0	0.5	1.0
4	0.9	1.0	0.1	0.3	0.2	0.9	1.0

(15) is automatically satisfied if (18) is satisfied. Compared with the literature, (15) and (18) can be regarded as generalized conditions for the weak and the strong string stability, respectively [17].

Focusing on the feasibility of implementation, i.e., for a platoon of heterogeneous vehicles with a limited communication structure and a decentralized control architecture, (18) is a useful condition to use in the controller design. Hence, in the rest of this paper, the sufficient condition (18) is considered as a necessary condition for string stability.

The string-stability transfer functions $\mathcal{G}_{U,i}(s)$, $\mathcal{G}_{X,i}(s)$, and $\mathcal{G}_{E,i}(s)$ directly follow from (17) and the schematic representation of the system in Fig. 6, yielding

$$\mathcal{G}_{U,i} = \frac{U_i}{U_{i-1}} = S_i(F_i D_i s^2 + K_i) G_{i-1}, \quad \text{for } i > 1 \tag{20a}$$

$$\mathcal{G}_{X,i} = \frac{X_i}{X_{i-1}} = S_i(F_i D_i s^2 + K_i) G_i, \quad \text{for } i > 1 \tag{20b}$$

$$\mathcal{G}_{E,i} = \frac{E_i}{E_{i-1}} = \begin{cases} S_2(1-\Xi_2) G_1 K_1, & \text{for } i = 2 \\ \frac{S_i(1-\Xi_i)}{S_{i-1}(1-\Xi_{i-1})} \frac{X_{i-1}}{X_{i-2}}, & \text{for } i > 2 \end{cases} \tag{20c}$$

where the dependency on the Laplace operator s is omitted for clarity, and

$$\Xi_i(s) = H_i(s) G_i(s) F_i(s) D_i(s) s^2, \qquad \text{for } i > \tag{21}$$

$$S_i(s) = \left(1 + H_i(s) G_i(s) K_i(s)\right)^{-1} \tag{22}$$

is the closed-loop sensitivity transfer function of vehicle i.

The transfer functions (20a)–(20c) are referred to as the input, the output, and the error string stability transfer functions, respectively. Strikingly, for homogeneous traffic, where $G_i(s) = G(s)$, and $K_i(s) = K(s)$, for $i > 1$, the string-stability transfer functions (20a)–(20c) are equal, i.e., $\mathcal{G}_{U,i}(s) = \mathcal{G}_{X,i}(s) = \mathcal{G}_{E,i}|_{i>2}(s)$. In the literature, homogeneous traffic is often considered, whereas the different string-stability transfer functions (20a)–(20c) are mixed up (e.g., see [8] and [19]). Focusing on heterogeneous traffic, where $G_i(s) \neq G_j(s)$, and $K_i(s) \neq K_j(s)$, for $i, j > 1$, $i \neq j$, the string-stability transfer functions (20a)–(20c) are clearly different.

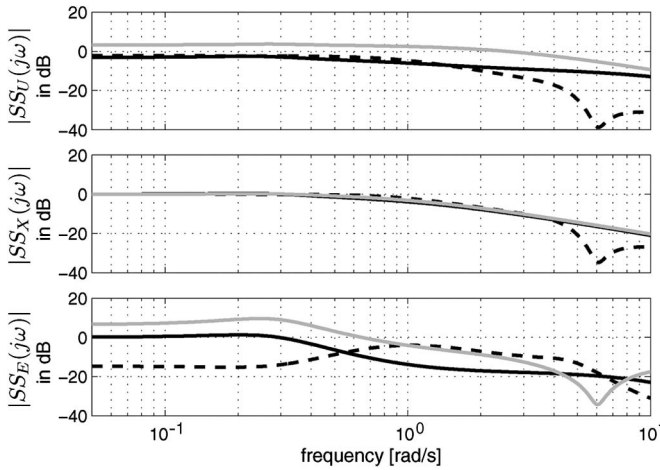

Fig. 7. Bode magnitude plots of the string-stability transfer functions (20a)–(20c), corresponding to three heterogeneous CACC-equipped vehicles $i \in \{2, 3, 4\}$ (solid black, dashed black, and solid grey, respectively), driving in a platoon. The system parameters for each vehicle are listed in Table I.

Consider a platoon of heterogeneous vehicles for which the system parameter values are given in Table I. Apart from the headway time, the parameters are chosen different for each vehicle. Substituting $G_i(s)$ (1), $K_i(s)$ (4), $H_i(s)$ (9), $D_i(s)$ (11), and $F_i(s)$ (13) in the string-stability transfer function (20) and using the system specifications in Table I yields the Bode magnitude plots shown in Fig. 7. As these plots show, the low-frequent asymptotic values of $|\mathcal{G}_{U,i}(j\omega)|$ and $|\mathcal{G}_{E,i}(j\omega)|$ differ per vehicle, whereas it is not the case for $|\mathcal{G}_{X,i}(j\omega)|$. Computing these values gives

$$\lim_{\omega \to 0} |\mathcal{G}_{U,i}(j\omega)| = \frac{k_{G_{i-1}}}{k_{G_i}}, \qquad \text{for } i > 1 \tag{23a}$$

$$\lim_{\omega \to 0} |\mathcal{G}_{X,i}(j\omega)| = 1, \qquad \text{for } i > 1 \tag{23b}$$

$$\lim_{\omega \to 0} |\mathcal{G}_{E,i}(j\omega)| = \begin{cases} \frac{\epsilon_2 k_{G_1} \omega_{K_1^2}}{k_{G_2} \omega_{K_2}^2}, & \text{for } i = 2 \\ \frac{\epsilon_i k_{G_{i-1}} \omega_{K_{i-1}^2}}{\epsilon_{i-1} k_{G_i} \omega_{K_i^2}}, & \text{for } i > 2 \end{cases} \tag{23c}$$

where

$$\epsilon_i = \lim_{\omega \to 0} |1 - \Xi_i(j\omega)| = 1 - \frac{k_{G_i}}{\hat{k}_{G_i}}, \qquad \text{for } i > 1 \tag{24}$$

with $\hat{k}_{G_i}$ being an estimate for $k_{G,i}$, which is used in the feedforward filter. In practice, $\hat{k}_{G_i} \neq k_{G_i}$ holds, yielding $\varepsilon_i \neq 0$ for $i > 1$.

As (23a) and (23c) show, the conditions for input and for error-string-stable behavior of vehicle i, for $i > 1$, depend on the characteristics of the dynamics of vehicle $i-1$. Without knowledge of these characteristics, no theoretical guarantees with regard to the input or error string stability can be given. Because these characteristics are not known *a priori*, the design of a string-stable CACC system is complicated, and probably, conservative performance requirements have to be adopted. Moreover, depending on the characteristics of the dynamics of vehicle $i-1$ with respect to the dynamics of vehicle i, it may be infeasible to guarantee input or error-string-stable behavior for vehicle i. For the output string-stability transfer function $\mathcal{G}_{X,i}(s)$, the string stability for vehicle i, $i > 1$ can be guaranteed, regardless of the dynamics of vehicle $i-1$. Based on this result, it is concluded that, for the CACC setup as presented in Section III and heterogeneous traffic, the output string stability has to be considered.

Correspondingly, the sufficient condition for string stability (18), with $\Lambda = X$, is adopted as a necessary condition for string stability (e.g., see [28]), yielding

$$\|\mathcal{G}_{X,i}(j\omega)\|_\infty = \left\| \frac{X_i(j\omega)}{X_{i-1}(j\omega)} \right\|_\infty \leq 1, \qquad \text{for } i > 1 \tag{25}$$

where $\mathcal{G}_{X,i}(s)$ is defined as in (20b), and $\|\mathcal{G}_{X,i}(j\omega)\|_\infty = 1$, for $i > 1$, $\omega > 0$, is denoted as the marginal string stability.

Note that this frequency-domain condition for string stability does not guarantee the absence of overshoot, considering the desired intervehicle distance, in the time domain (e.g., see [19] and [21]).

V. System Analysis That Focuses on String Stability

Consider the CACC system setup as presented in Section III, with the feedback controller $K_i(s)$ in (4), the feedforward filter $F_i(s)$ in (13), and the spacing policy dynamics $H_i(s)$ in (9). Furthermore, assume that the low-level longitudinal vehicle dynamics (1) are ideal, yielding $G_i(s) = s^{-2}$. Hence, the design variables are the feedback controller breakpoint frequency $\omega_{K,i}$, the feedforward filter $F_i(s)$, and the headway time $h_{d,i}$.

In this section, the influence of these design variables on the string stability of the proposed CACC systems setup is analyzed for these idealized vehicle dynamics. Experimental validation with real nonideal vehicle dynamics is discussed in the next section. Note that the string-stability transfer function (20b) and, hence, the string-stability condition (25) are independent of the dynamics of other vehicles in the platoon. Consequently, although idealized vehicle dynamics are considered, the analysis holds for homogeneous and heterogeneous traffic.

A. Constant Velocity-Independent Intervehicle Spacing

Lemma 5.1: Consider the control setup as presented in Section III, i.e., the ideal vehicle dynamics $G_i(s) = s^{-2}$, and assume that a controller $K_i(s)$ with $\omega_{K,i} > 0$ is designed, which renders the corresponding closed-loop $T_i'(s)$ (2) stable, where the corresponding open-loop $L_i'(s) = K_i(s)G_i(s)$ is a proper transfer function. Given the string-stability condition (25), only the marginal string stability can be guaranteed for a constant velocity-independent intervehicle spacing, i.e., $h_{d,i} = 0.0$ s.

Proof: To start with, consider the case of no feedforward, i.e., $F_i(s) = 0$. Without feedforward, an ACC system, instead of a CACC system, results. A constant velocity-independent intervehicle spacing implies $h_{d,i} = 0.0$ s, yielding $H_i(s) = 1$. Correspondingly, the output string-stability transfer function (20b) reduces to

$$\mathcal{G}_{X,i}(s) = \frac{G_i(s)K_i(s)}{1 + G_i(s)K_i(s)} = T_i'(s), \qquad \text{for } i > 1 \tag{26}$$

where $T_i'(s)$ is the complementary sensitivity of the inner control loop (see Section III-A). If $T_i'(s)$ is stable and the corresponding open-loop $L_i'(s) = K_i(s)G_i(s)$ is a proper transfer function, it holds that, if the magnitude of $T_i'(s)$ is smaller than 1 over some frequency range, it will always be larger than 1 in another frequency range, which is due to the well-known Bode-sensitivity-integral constraint [31], [32]. Hence, only the marginal string stability can be guaranteed, $\|T_i'(j\omega)\|_\infty = |T_i'(j\omega)| = 1$, for $i > 1$, $\omega > 0$.

Next, consider the case with the feedforward filter $F_i(s)$, as defined in (13). If the communication delay equals $\theta_i = 0.0$ s, yielding $D_i(s) = 1$, the string-stability transfer function (20b) becomes

$$\mathcal{G}_{X,i}(s) = \frac{1 + G_i(s)K_i(s)}{1 + G_i(s)K_i(s)} = 1, \qquad \text{for } i > 1. \tag{27}$$

Hence, in that case, only the marginal string stability $\|\mathcal{G}_{X,i}(j\omega)\|_\infty = 1$, for $i > 1$, $\omega > 0$, can be guaranteed. If a communication delay $\theta_i > 0.0$ s is present, the string stability condition (25) becomes

$$\left| \frac{D_i(j\omega) + G_i(j\omega)K_i(j\omega)}{1 + G_i(j\omega)K_i(j\omega)} \right| \leq 1, \qquad \text{for } i > 1, \forall\omega. \tag{28}$$

Substituting $D_i(j\omega)$ (11) and, without loss of generality, $G_i(j\omega)K_i(j\omega) = f_i(\omega) + j\, g_i(\omega)$, gives, for $i > 1, \forall\, \omega$

$$\left| e^{-\theta_i j\omega} + f_i(\omega) + j\, g_i(\omega) \right| \leq |1 + f_i(\omega) + j\, g_i(\omega)| \tag{29}$$

which yields, for $i > 1, \forall\, \omega$

$$\begin{cases} \frac{g_i(\omega)}{f_i(\omega)} \sin(-\theta_i\omega) & \leq & 1 - \cos(-\theta_i\omega), & \text{for } f_i(\omega) > 0 \\ 2g_i(\omega) \sin(-\theta_i\omega) & \leq & 0, & \text{for } f_i(\omega) = 0 \\ \frac{g_i(\omega)}{f_i(\omega)} \sin(-\theta_i\omega) & \geq & 1 - \cos(-\theta_i\omega), & \text{for } f_i(\omega) < 0. \end{cases} \tag{30}$$

Standard goniometry shows that (30) is only true for $f_i(\omega) \geq 0$ and $g_i(\omega) = 0$. Moreover, in that case, only the marginal string stability can be guaranteed. In all other cases, string stability cannot be guaranteed. ■

B. Velocity-Dependent Intervehicle Spacing: ACC Case

Lemma 5.2: Consider the ACC control setup as presented in Section III-B, and the ideal vehicle dynamics $G_i(s) = s^{-2}$.

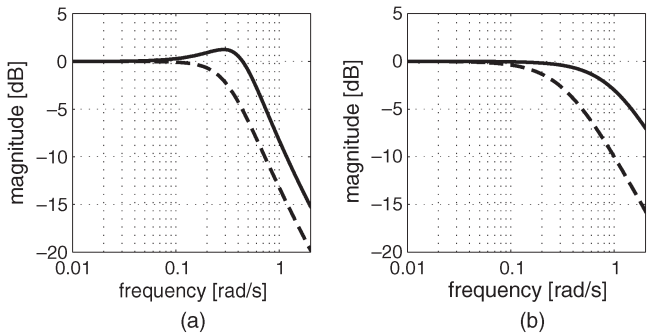

Fig. 8. Bode magnitude plots of $\mathcal{G}_{X,i}(j\omega)$ (20b), corresponding to (a) the ACC case, and (b) the CACC case, for $h_{d,i} = 1.0$ s (solid black), and $h_{d,i} = 3.0$ s (dashed black).

Given the string-stability condition (25), string stability can be guaranteed for $h_{d,i} \geq h_{d,i,\min}(\omega_{K,i})$.

Proof: In the case of an ACC system, no feedforward is present, i.e., $F_i(s) = 0$. For $h_{d,i} > 0.0$ s, the output string-stability transfer function (20b) equals

$$\mathcal{G}_{X,i}(s) = \frac{G_i(s)K_i(s)}{1 + H_i(s)G_i(s)K_i(s)}, \qquad \text{for } i > 1. \tag{31}$$

Substituting $G_i(s) = s^{-2}$, $K_i(s)$ (4), and $H_i(s)$ (9), in (31), the string-stability condition (25) yields

$$\frac{\omega_{K,i}^2\left(2 - \omega_{K,i}^2 h_{d,i}^2\right)}{(1 + \omega_{K,i}h_{d,i})^2} \leq \omega^2, \qquad \text{for } i > 1, \forall\omega. \tag{32}$$

Because $\omega \in \mathbb{R}^+$ holds, this expression implies $\min\{\omega^2\} = 0$, leading to

$$\frac{\omega_{K,i}^2\left(2 - \omega_{K,i}^2 h_{d,i}^2\right)}{(1 + \omega_{K,i}h_{d,i})^2} \leq 0, \qquad \text{for } i > 1. \tag{33}$$

Because $\omega \in \mathbb{R}^+$ holds, this expression implies $\min\{\omega^2\} = 0$, and it directly follows that string stability can be guaranteed for

$$h_{d,i} \geq h_{d,i,min} = \sqrt{2}\omega_{K,i}^{-1}, \qquad \text{for } i > 1. \tag{34}$$

■

Example: Take $\omega_{K,i} = 0.5$ rad/s. Consider the ideal vehicle dynamics $G_i(s) = s^{-2}$, implying $k_{G,i} = 1.0$, $\tau_i = 0$, and $\phi_i = 0.0$ s. The bandwidth $\omega'_{bw,i}$ and the phase margin $\alpha'_{PM,i}$ that correspond to $T'_i(s)$ are then straightforwardly derived as $\omega'_{bw,i} \approx 0.6$ rad/s and $\alpha'_{PM,i} \approx 51^\circ$, respectively (see Section III). Following (34), $h_{d,i} \geq h_{d,i,\min} \approx 2.8$ s has to hold to ensure string stability, as illustrated in Fig. 8(a), showing the corresponding Bode magnitude plots of $\mathcal{G}_{X,i}(j\omega)$.

C. Velocity-Dependent Intervehicle Spacing: CACC Case

Lemma 5.3: Consider the control setup as presented in Section III-C, ideal vehicle dynamics $G_i(s) = s^{-2}$, and a specific operating range $(\omega_{K,i}, \theta_i) \in \Omega_K \times \Theta = [0.1, 2.0]$ rad/s $\times$ $[0.0, 0.5]$ s, $i > 1$. Given the string-stability condition (25), string stability can be guaranteed for $h_{d,i} \geq h_{d,i,\min}(\omega_{K,i}, \theta_i)$.

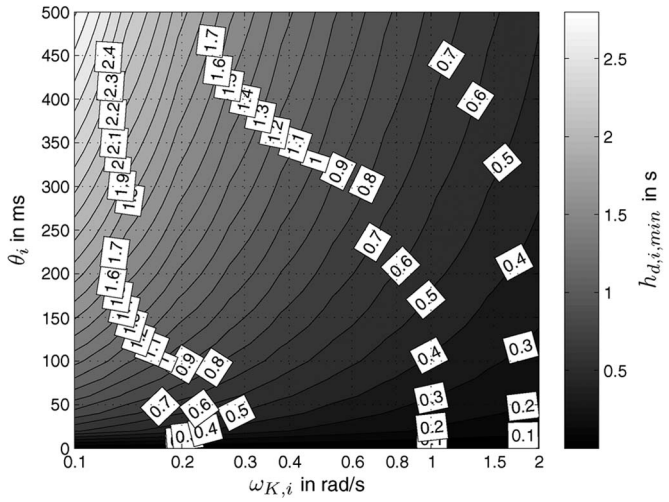

Fig. 9. Contour plot of $\omega_{K,i}$ versus θ_i, indicating the corresponding minimal value for $h_{d,i,\min}(\omega_{K,i}, \theta_i)$ for which string stability is ensured.

Proof: Substituting the feedforward filter $F_i(s)$ (13) in (20b) yields

$$\mathcal{G}_{X,i}(s) = \frac{D_i(s) + H_i(s)G_i(s)K_i(s)}{H_i(s)\left(1 + H_i(s)G_i(s)K_i(s)\right)}, \qquad \text{for } i > 1. \tag{35}$$

In the case of no communication delay, i.e., $\theta_i = 0.0$ s, yielding $D_i(s) = 1$, (35) reduces to

$$\mathcal{G}_{X,i}(s) = \frac{1}{H_i(s)}, \qquad \text{for } i > 1. \tag{36}$$

Hence, for a velocity-dependent intervehicle spacing with $h_{d,i} > 0.0$ s, the string-stability condition (25) is directly fulfilled.

If a communication delay $\theta_i > 0.0$ s is taken into account, the analytical derivation of the minimal required headway time $h_{d,i,\min}$ becomes rather complex and does not provide additional insight. Consequently, this derivation is not discussed here. Instead, in Fig. 9, the results of a numerical approximation of $h_{d,i,\min} = h_{d,i,\min}(\omega_{K,i}, \theta_i)$ are shown for $(\omega_{K,i}, \theta_i) \in \Omega_K \times \Theta = [0.1, 2.0]$ rad/s $\times$ $[0.0, 0.5]$ s. The results in Fig. 9 show that, depending on $\omega_{K,i}$ and on the size of the time delay in the wireless communication signal θ_i, string stability is guaranteed for $h_{d,i} > h_{d,i,\min}(\omega_{K,i}, \theta_i)$, where, following (36), $\lim_{\theta_i \to 0} h_{d,i,\min}(\omega_{K,i}, \theta_i) = 0.0$ s holds. ■

If $\omega_{K,i}$ and θ_i are known, the minimum value $h_{d,i} = h_{d,i,\min}(\omega_{K,i}, \theta_i)$ required to guarantee string stability in the case of a CACC system directly follows from Fig. 9. Both the results in Fig. 9 and the result in (34) clearly depend on the design of $K_i(s)$. Moreover, the result only holds for the ideal vehicle dynamics and the spacing policy dynamics as defined in (6). A different design of $K_i(s)$ for non-ideal vehicle dynamics $G_i(s)$ or a different choice for $x_{r,d,i}(t)$ would yield different results. Hence, note that the minimal headway time as presented in Fig. 9 and the result (34) does not reflect the absolute minimum that is feasible with the proposed ACC setup. Nevertheless, comparing the result in Fig. 9 with the minimal headway time that is required in the case of an ACC system (34) for a reasonably valued delay time θ_i, the minimal

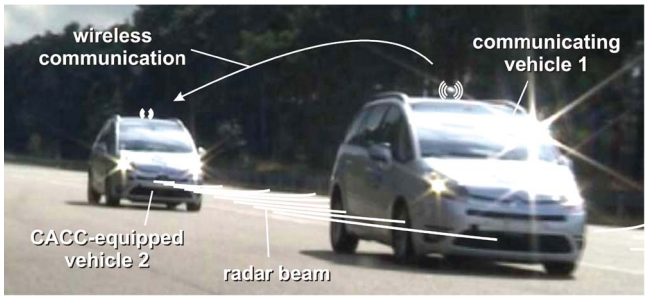

Fig. 10. Experimental setup with two Citroën C4s [33].

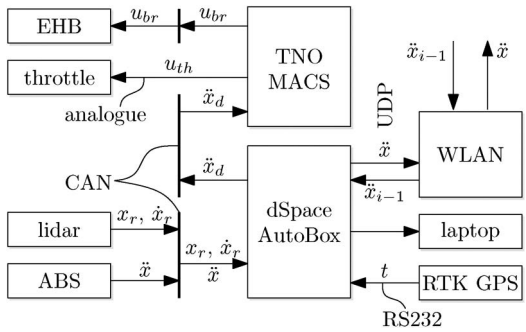

Fig. 11. Schematic overview of the instrumentation of the vehicles. The main communication channels and corresponding signals are indicated, where $u_{\mathrm{th}}(t)$ and $u_{br}(t)$ are the throttle and brake system control signals, respectively, $\ddot{x}_d(t)$ and $\ddot{x}(t)$ are the desired and actual acceleration, respectively, $x_r(t)$ and $\dot{x}_r(t)$ are the relative position and velocity, respectively, $\ddot{x}_{i-1}(t)$ is the communicated acceleration of the preceding vehicle, and t is the time stamping signal. For clarity, both the index i, indicating vehicle i, and the time dependency of the signals are omitted.

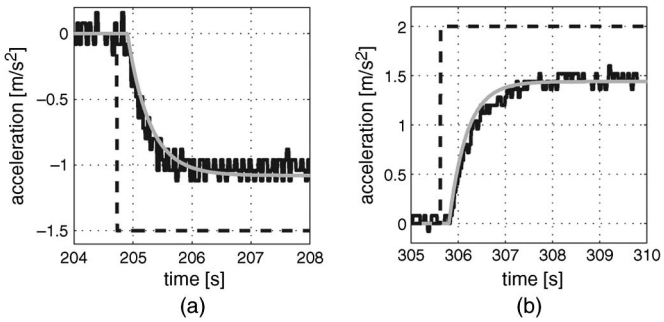

Fig. 12. Identification step-response measurement results for (a) braking and (b) accelerating. The reference step input (dashed black), the measurement results (solid black), and the corresponding simulation results with the model $G_i^*(s) = G_i(s)s^2$ (solid grey) are shown.

headway time required to guarantee string stability in case of a CACC system is significantly smaller.

Example: Take $\theta = 200$ ms and, analogous to the example in Section V-B, $\omega_{K,i} = 0.5$ rad/s. Fig. 9 indicates that string stability can be guaranteed for $h_{d,i} \gtrapprox 0.8$ s. This value is clearly smaller than the minimum value required to achieve string stability in the case of an ACC system, which is $h_{d,i,\min} \approx 2.8$ s (see Section V-B). The corresponding Bode magnitude plot of $\mathcal{G}_{X,i}(j\omega)$ for $h_{d,i} = 1.0$ s is shown in Fig. 8(b), confirming this result.

VI. Experimental Validation

To validate the theory, experiments are performed using two vehicles. The models for the communication delay and the vehicle dynamics are identified using measurements. Based on these models, the designs of the feedback controller, the feedforward filter, and the spacing policy dynamics are discussed. Three different experiments are executed, including experiments with and without wireless communication and experiments with different headway times [33].

A. Experimental Setup

Two Citroën C4s are used as a testing platform (see Fig. 10). For the wireless intervehicle communication, the standard Wi-Fi protocol IEEE 802.11g is used, with an update rate of 10 Hz [34]. The acceleration of vehicle 1 is derived from the built-in antilock braking system (ABS), which is available on the controller area network (CAN-bus), and is communicated to vehicle 2. A zero-order-hold approach is adopted for the communicated signal, introducing a corresponding average delay of about 50 ms. To synchronize the measurements of the two vehicles, the Global Positioning System (GPS) time stamping is adopted. Correspondingly, an additional communication delay of about 10 ms is identified. Combination of these values yields $\theta_i \approx 60$ ms as a total delay for the model $D_i(s)$ (11).

Vehicle 2 is equipped with an electrohydraulic braking (EHB) system, facilitating brake-by-wire control. Implementation of the controller for the longitudinal dynamics of the vehicle and actuation of the throttle and EHB system are covered by the Netherlands Organization for Applied Scientific Research (TNO) modular automotive control system (MACS) [35]. An OMRON laser radar, i.e., a lidar, with a 150-m range is built in. Using rapid control prototyping, the CACC system is implemented on a dSpace AutoBox, with a sample rate of 100 Hz. Finally, a laptop is used to monitor all signals and to log the data. A schematic overview of the instrumentation is shown in Fig. 11.

B. Vehicle Model Identification

In the system analysis presented in Section V, it is assumed that the low-level closed-loop dynamics of the vehicle $G_i(s)$ (1) are ideal, i.e., $G_i(s) = s^{-2}$. In practice, however, this condition does not hold. Open-loop step-response measurements are performed to identify these dynamics. Measurements are performed for various acceleration levels and at different velocities. A least squares minimization method is used to identify the parameters of the model for the vehicle dynamics (1). This identification results in a bandwidth $\omega_{bw,l,i} = \tau_i^{-1} = 0.38$ rad/s, a delay time $\phi_i = 0.18$ s, and a system gain $k_{G,i} = 0.72$. Two of the measurement results and corresponding simulation results with the identified model $G_i^*(s) = G_i(s)s^2$ are shown in Fig. 12.

Comparing the measurement and the simulation results shows that the model appropriately represents the longitudinal vehicle dynamics. The same holds for validation measurements, of which an example is shown in Fig. 13(a). Hence, the proposed model structure for $G_i(s)$ (1) is sufficient to describe the low-level vehicle dynamics. The main differences between the identified vehicle model $G_i(s)$ and the ideal vehicle dynamics

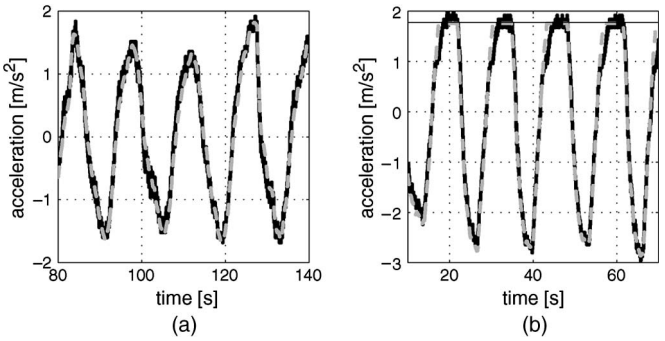

Fig. 13. Validation measurement results for the identified vehicle model (a) without and (b) with saturation. The measured acceleration (solid black), the simulated model response (dashed grey), and the saturation limit (solid black) are shown. The simulated response covers most of the measured acceleration signal. The desired acceleration is omitted for clarity.

considered in the system analysis of Section V are in the low-frequent gain, i.e., $k_{G,i} \neq 1.0$, and the actuator delay, i.e., $\phi_i \neq 0.0$ s. The consequences of these differences will later be evaluated.

Attention should be paid to the size of the acceleration signal. Measurements show that the acceleration saturates at about 1.8 m/s^2. Simulation results show that the model $G_i^*(s)$, including this saturation, appropriately represents the saturated vehicle dynamics [see Fig. 13(b)]. However, nonlinearities, such as this saturation, are not accounted for in the presented frequency-domain CACC design and the corresponding string-stability analysis. Hence, to validate the theory presented in Section V, it has been ensured that the desired acceleration does not exceed this saturation limit during the experiments.

C. CACC Design

The CACC design follows the setup as proposed in Section V. The implemented feedback controller $K_i(s)$ is a combination of the PD controller (4) and a first-order low-pass filter to prevent amplification of high-frequent noise, which is present in the lidar measurements. Furthermore, for comparison with the results of the previous section, the identified low-frequent gain $k_{G,i}$ is compensated for by adjusting the proportional action, yielding

$$K_i(s) = \frac{\omega_{K,i}}{k_{G,i}} \frac{\omega_{K,i} + s}{\omega_{f,i} + s}, \qquad \text{for } i > 1 \tag{37}$$

where $\omega_{f,i}$ is the cutoff frequency of the low-pass filter, which equals half the sample frequency, i.e., $\omega_{f,i} = 100.0\pi$ rad/s. Analogous to the example in Section V-B, $\omega_{K,i} = 0.5$ rad/s is used. Combining the resulting controller with the identified vehicle model yields a closed-loop bandwidth of $\omega'_{bw,i} \approx 0.6$ rad/s, with a phase margin $\alpha'_{PM,i} \approx 1.0$ rad/s $\approx 30°$. Hence, a reasonable phase margin results, and moreover, $\omega_{bw,l,i} > \omega'_{bw,i}$ holds (see Section VI-B). This result indicates that the design is robustly stable and that the tracking performance is not degraded by the low-level longitudinal dynamics.

For the feedforward controller $F_i(s)$, the design as proposed in (13) is used, where the identified model for the low-level longitudinal vehicle dynamics is used (see Section VI-B). For the spacing policy, an additional low-pass filter is used to filter the velocity measurements of the lidar, which are used to compute the desired intervehicle distance $x_{r,d,i}(t)$ in (6). The cutoff frequency of the low-pass filter is chosen to be about ten times larger than the bandwidth of the inner loop bandwidth, i.e., 5.0 rad/s. Taking a higher cutoff frequency has no practical relevance, because the inner control loop cannot track the corresponding desired relative position $x_{r,d,i}(t)$. A lower cutoff frequency would result in too much phase lag.

TABLE II
OVERVIEW OF THE EXPERIMENTS, WHERE $h_{d,i,\min}$ IS THE MINIMAL HEADWAY TIME REQUIRED FOR STRING STABILITY, AND $h_{d,i}$ IS THE HEADWAY TIME USED IN THE EXPERIMENTS

Experiment	communication	$h_{d,i,min}$ in s	$h_{d,i}$ in s
i	no	2.6	3.0
ii	no	2.6	1.0
iii	yes	0.8	1.0

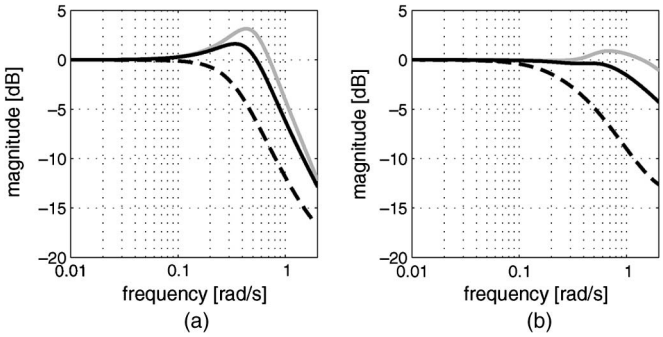

Fig. 14. Bode magnitude plots of $\mathcal{G}_{X,i}(j\omega)$ in (35) in the case of (a) ACC and (b) CACC for $h_{d,i} = 0.5$ s (solid grey), $h_{d,i} = 1.0$ s (solid black), and $h_{d,i} = 3.0$ s (dashed black).

D. String-Stability Experiments

To validate the theory in Section V, three experiments are performed, which are listed in Table II: 1) a system using wireless communication (CACC); 2) a system without using wireless communication (ACC); and 3) a system for different headway times $h_{d,i}$.

Using the string-stability condition (25), the minimal headway times that are required to ensure string stability in the case of ACC and CACC are numerically computed as $h_{d,i,\min} = 2.6$ and 0.8 s, respectively. In Fig. 14, the Bode magnitude plots of the string-stability transfer function $\mathcal{G}_{X,i}(s)$ (20b) are shown for $h_{d,i} \in \{0.5, 1.0, 3.0\}$ s. The Bode plots confirm the numerical results, indicating string stability both in the case of ACC with a headway time, i.e., $h_{d,i} = 3.0 > 2.6$ s, and in the case of CACC with a headway time, i.e., $h_{d,i} \in \{1.0, 3.0\} > 0.8$ s. However, both in the case of ACC with a headway time $h_{d,i} \in \{0.5, 1.0\} < 2.6$ s and in the case of CACC with a headway time of $h_{d,i} = 0.5 < 0.8$ s, the string-stability condition is not fulfilled. Consequently, string-stable driving behavior is expected in both experiments 1 and 3, whereas string-unstable behavior is expected in experiment 2.

Comparing the Bode magnitude plots in Figs. 8 and 14 shows that, in this case, the influence of the nonideal vehicle dynamics on the string stability transfer functions is small. This condition can be attributed to the compensation for the vehicle model gain in the feedback controller [see (37)] and the relatively small

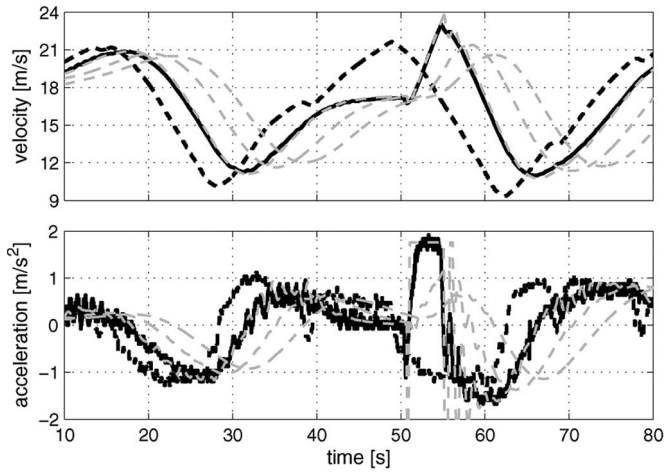

Fig. 15. Measurement results of Experiment i (see Table II). In the upper figure, the measured velocities of vehicle 1 (dashed black) and vehicle 2 (solid black), as well as the resulting velocities for the three simulated vehicles (dashed grey) are shown. In the bottom figure, the corresponding acceleration signals are shown.

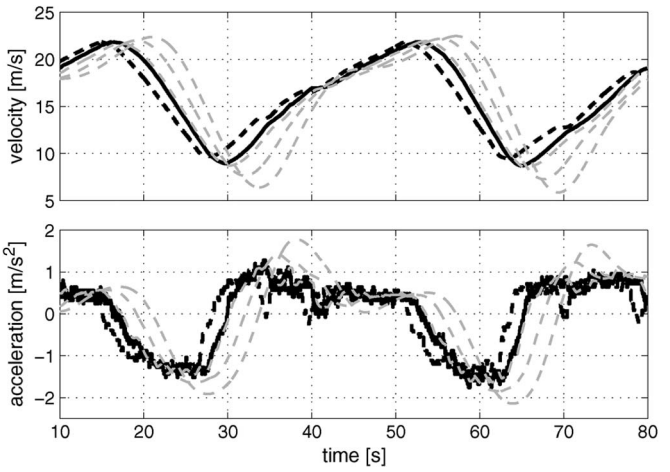

Fig. 16. Measurement results of Experiment ii (see Table II). In the upper figure, the measured velocities of vehicle 1 (dashed black) and vehicle 2 (solid black), as well as the resulting velocities for the three simulated vehicles (dashed grey) are shown. In the bottom figure, the corresponding acceleration signals are shown.

communication delay (see Section VI-B). The main difference can be related to a relatively large actuator delay $\phi_i = 0.18$ s (see Section VI-B).

The experiments are performed with two vehicles (see Fig. 10). To increase insight into the measurement results, the response of vehicle 2 is also simulated offline. Analogously, the platoon is virtually extended by simulating an additional two vehicles $i \in \{3, 4\}$. For the simulations, a model that includes saturation is used (see Fig. 13). The input for the simulated vehicle 2 is derived from the communicated acceleration of vehicle 1. Furthermore, for this purpose, the velocity of vehicle 1 is also obtained through wireless communication. The input for the subsequent vehicles directly follows from the simulated vehicle 2. For clarity, homogeneous traffic is considered, i.e., identical vehicle models, identical feedback and feedforward controllers, and identical headway times are used.

In both experiments 1 and 2, wireless communication is not used, which means that an ACC system results. In Figs. 15 and 16, measurement results and corresponding simulation results for experiments 1 and 2 are shown. For experiment 1, the amplitude of the oscillations in the velocity and the acceleration of vehicle 2 is smaller than for vehicle 1, which corresponds to the anticipated string-stable behavior. The results of the simulated vehicles confirm this conclusion. Moreover, the resemblance between the measurement results and the simulated vehicle 2 is good, validating the use of the simulation results. The peak in the measured velocity and acceleration at about 55 s is a result of a loss of the fix of the lidar, resulting in a switch to the standard cruise control functionality and maximum acceleration.

For experiment 2, the behavior of vehicle 2 is, as expected, string unstable, i.e., the oscillations in the velocity of vehicle 1 are amplified by vehicle 2. Again, the resemblance between the simulated vehicle 2 and the measurement results is good, validating the use of the results of the simulated vehicles to emphasize this observation. The results of this experiment validate the observation that the use of the standard ACC functionality

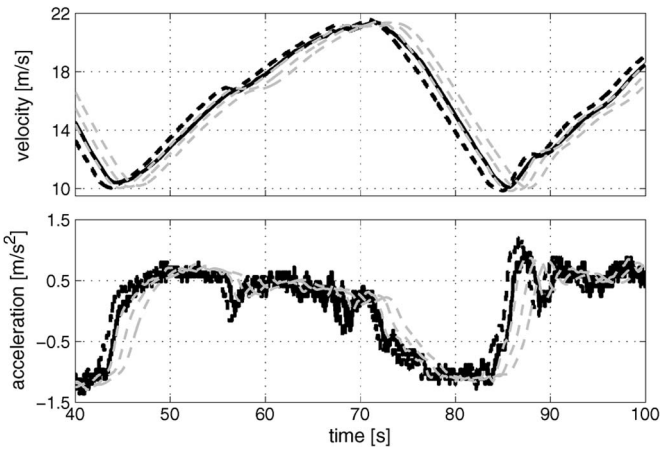

Fig. 17. Measurement results of Experiment iii (see Table II). In the upper figure, the measured velocities of vehicle 1 (dashed black) and vehicle 2 (solid black), as well as the resulting velocities for the three simulated vehicles (dashed grey) are shown. In the bottom figure, the corresponding acceleration signals are shown.

while driving at smaller intervehicle distances induces string-unstable behavior, which, for example, results in traffic jams (see Section I).

In Fig. 17, measurement and simulation results for experiment 3 are shown. The wireless information is used, yielding a true CACC system. As anticipated, the behavior of vehicle 2 is string stable, which is confirmed by the simulation results. Comparing the results for the ACC system in experiment 2 and the CACC system in experiment 3 validates the conclusion that, given the proposed CACC system setup, the minimal headway time required to guarantee string stability is smaller in the case of CACC, which is enabled by the wireless communication link. Moreover, comparing the results of the ACC experiments and the CACC experiments shows that the tracking performance is significantly improved in the case of a CACC system. Considering that the main difference between the ACC and CACC system is a feedforward filter, this result is expected.

VII. Conclusion and Future Work

The design of a CACC system that focuses on the feasibility of implementation has been presented. A communication link with the directly preceding vehicle was considered, communication delay and heterogeneity of the traffic was taken into account, a decentralized controller design was adopted, and using a feedforward controller design, the system can easily degrade to a standard ACC system in case wireless communication is not available or fails.

Based on this setup, the string-stability characteristics of the CACC system are analyzed using a frequency-domain-based approach. This analysis yields the following conclusions.

- Output string stability has to be considered when heterogeneous traffic is taken into account.
- A velocity-dependent spacing policy is required to achieve string-stable system behavior.
- The CACC feedforward controller enables small intervehicle distances while maintaining string stability, whereas this is not the case for the standard ACC feedback controller alone.

Experimental results with two CACC-equipped vehicles validate these theoretical results. The experimental results illustrate that, with a relatively simple CACC system setup, which focuses on the feasibility of implementation, significant improvements with regard to the minimal headway time and string-stability characteristics can be achieved with respect to a standard ACC system.

Further experimental validation of the concept using a larger string of vehicles should be a subject for future research. In addition, comparison of the performance and string-stability characteristics of the proposed system setup with different CACC setups is an interesting issue for further research. For example, setups that adopt different communication structures or different spacing policy dynamics can be compared. Finally, important issues for future research should include both saturations and robustness against model uncertainties and disturbances in the string-stability analysis and consideration of the behavior of mixed strings with both CACC-equipped vehicles and nonequipped normal traffic.

References

[1] *Transport Information and Control Systems—Adaptive Cruise Control Systems: Performance Requirements and Test Procedures*, NEN-ISO 15622, 2002.

[2] P. A. Ioannou and C. C. Chien, "Autonomous intelligent cruise control," *IEEE Trans. Veh. Technol.*, vol. 42, no. 4, pp. 657–672, Nov. 1993.

[3] A. Vahidi and A. Eskandarian, "Research advances in intelligent collision avoidance and adaptive cruise control," *IEEE Trans. Intell. Transp. Syst.*, vol. 4, no. 3, pp. 143–153, Sep. 2003.

[4] B. van Arem, C. J. G. van Driel, and R. Visser, "The impact of cooperative adaptive cruise control on traffic flow characteristics," *IEEE Trans. Intell. Transp. Syst.*, vol. 7, no. 4, pp. 429–436, Dec. 2006.

[5] S. E. Shladover, "Automated vehicles for highway operations (automated highway systems)," *Proc. Inst. Mech. Eng. I: J. Syst. Control Eng.*, vol. 219, no. 1, pp. 53–75, Nov. 2005.

[6] L. Peppard, "String stability of relative-motion PID vehicle control systems," *IEEE Trans. Autom. Control*, vol. AC-19, no. 5, pp. 579–581, Oct. 1974.

[7] Y. Sugiyama, M. Fukui, M. Kikuchi, K. Hasebe, A. Nakayama, K. Nishinari, S. Tadaki, and S. Yukawa, "Traffic jams without bottlenecks—Experimental evidence for the physical mechanism of the formation of a jam," *New J. Phys.*, vol. 10, no. 3, p. 033 001, Mar. 2008.

[8] R. Rajamani and C. Zhu, "Semiautonomous adaptive cruise control systems," *IEEE Trans. Veh. Technol.*, vol. 51, no. 5, pp. 1186–1192, Sep. 2002.

[9] X. Y. Lu, S. Shladover, and J. K. Hedrick, "Heavy-duty truck control: Short intervehicle distance following," in *Proc. Amer. Control Conf.*, Boston, MA, Jul. 2004, vol. 5, pp. 4722–4727.

[10] S. Sheikholeslam and C. A. Desoer, "A system-level study of the longitudinal control of a platoon of vehicles," *Trans. ASME: J. Dyn. Syst. Meas. Control*, vol. 114, no. 2, pp. 286–292, Jun. 1992.

[11] D. Swaroop, J. K. Hedrick, and S. B. Choi, "Direct adaptive longitudinal control of vehicle platoons," *IEEE Trans. Veh. Technol.*, vol. 50, no. 1, pp. 150–161, Jan. 2001.

[12] G. J. L. Naus, R. P. A. Vugts, J. Ploeg, M. J. G. van de Molengraft, and M. Steinbuch, "Towards on-the-road implementation of cooperative adaptive cruise control," in *Proc. 16th World Congr. Exhib. Intell. Transp. Syst. Serv.*, Stockholm, Sweden, Sep. 2009.

[13] W. Levine and M. Athans, "On the optimal error regulation of a string of moving vehicles," *IEEE Trans. Autom. Control*, vol. AC-11, no. 3, pp. 355–361, Jul. 1966.

[14] D. Yanakiev and I. Kanellakopoulos, "Nonlinear spacing policies for automated heavy-duty vehicles," *IEEE Trans. Veh. Technol.*, vol. 47, no. 4, pp. 1365–1377, Nov. 1998.

[15] S. Sheikholeslam and C. A. Desoer, "Longitudinal control of a platoon of vehicles with no communication of lead vehicle information: A system-level study," *IEEE Trans. Veh. Technol.*, vol. 42, no. 4, pp. 546–554, Nov. 1993.

[16] K. Santhanakrishnan and R. Rajamani, "On spacing policies for highway vehicle automation," *IEEE Trans. Intell. Transp. Syst.*, vol. 4, no. 4, pp. 198–204, Dec. 2003.

[17] D. Swaroop, J. K. Hedrick, C. C. Chien, and P. A. Ioannou, "A comparison of spacing and headway control strategy for automatically controlled vehicles," *Veh. Syst. Dyn.*, vol. 23, no. 8, pp. 597–625, Nov. 1994.

[18] P. Barooah and J. P. Hespanha, "Error amplification and disturbance propagation in vehicle strings with decentralized linear control," in *Proc. 44th IEEE Conf. Decis. Control*, Dec. 2005, pp. 4964–4969.

[19] D. Swaroop and J. K. Hedrick, "Constant spacing strategies for platooning in automated highway systems," *Trans. ASME: J. Dyn. Syst. Meas. Control*, vol. 121, no. 3, pp. 462–470, Sep. 1999.

[20] E. Shaw and J. K. Hedrick, "Controller design for string stable heterogeneous vehicle strings," in *Proc. 46th IEEE Conf. Decis. Control*, Dec. 2007, pp. 2868–2875.

[21] M. E. Khatir and E. J. Davison, "Decentralized control of a large platoon of vehicles using nonidentical controllers," in *Proc. Amer. Control Conf.*, Boston, MA, Jul. 2004, pp. 2769–2776.

[22] X. Liu and S. S. Mahal, "Effects of communication delay on string stability in vehicle platoons," in *Proc. IEEE Intell. Transp. Syst. Conf.*, Aug. 2001, pp. 625–630.

[23] P. Seiler, A. Pant, and J. K. Hedrick, "Disturbance propagation in vehicle strings," *IEEE Trans. Autom. Control*, vol. 49, no. 10, pp. 1835–1841, Oct. 2004.

[24] S. E. Shladover, C. A. Desoer, J. K. Hedrick, M. Tomizuka, J. Walrand, W.-B. Zhang, D. H. McMahon, H. Peng, S. Sheikholeslam, and N. McKeown, "Automated vehicle control developments in the PATH program," *IEEE Trans. Veh. Technol.*, vol. 40, no. 1, pp. 114–130, Feb. 1991.

[25] S. C. Warnick and A. A. Rodriguez, "Longitudinal control of a platoon of vehicles with multiple saturating nonlinearities," in *Proc. Amer. Control Conf.*, Baltimore, MD, Jun. 1994, vol. I, pp. 403–407.

[26] R. Rajamani, S. B. Choi, B. K. Law, J. K. Hedrick, R. Prohaska, and P. Kretz, "Design and experimental implementation of longitudinal control for a platoon of automated vehicles," *Trans. ASME: J. Dyn. Syst. Meas. Control*, vol. 122, no. 3, pp. 470–476, Sep. 2000.

[27] C. Y. Liang and H. Peng, "Adaptive cruise control with guaranteed string stability," *Veh. Syst. Dyn.*, vol. 32, no. 4/5, pp. 313–330, Nov. 1999.

[28] X. Huppe, J. D. Lafontaine, M. Beauregard, and F. Michaud, "Guidance and control of a platoon of vehicles adapted to changing environment conditions," in *Proc. IEEE Int. Conf. Syst., Man, Cybern.*, Oct. 2003, vol. 4, pp. 3091–3096.

[29] E. Shaw and J. K. Hedrick, "String stability analysis for heterogeneous vehicle strings," in *Proc. Amer. Control Conf.*, New York, Jul. 2007, pp. 3118–3125.

[30] C. Y. Liang and H. Peng, "String stability analysis of adaptive cruise controlled vehicles," *JSME Int. J. Mech. Syst., Mach. Elements Manuf.*, vol. 43, no. 3, pp. 671–677, Sep. 2000.

[31] M. M. Seron, J. H. Braslavsky, and G. C. Goodwin, *Fundamental Limitations in Filtering and Control*. London, U.K.: Springer-Verlag, 1997.

[32] H. W. Bode, *Network Analysis and Feedback Amplifier Design*. New York: Van Nostrand, 1945.
[33] G. J. L. Naus, R. P. A. Vugts, J. Ploeg, M. J. G. van de Molengraft, and M. Steinbuch, CACC String Stability Tests, Sep. 2009. [Online]. Available: http://www.youtube.com/watch?v=aNYh4MjeSpU
[34] I. C. Society, IEEE Std. 802.11g (TM), New York, Jun. 2003.
[35] TNO Automotive, Modular Automotive Control System (MACS), Aug. 2009. [Online]. Available: http://www.tno.nl/automotive

Gerrit J. L. Naus received the M.Sc. degree in mechanical engineering from Eindhoven University of Technology, Eindhoven, The Netherlands, in 2005. His graduation project was performed at Fontijne Grotnes B.V., Vlaardingen, The Netherlands, at which, after receiving the M.Sc. degree, he continued working for five months as a Development Engineer with the R&D Department. Since 2006, he has been working toward the Ph.D. degree with the Control Systems Technology Group, Department of Mechanical Engineering, Eindhoven University of Technology. His Ph.D. study is focused on model-based control for automotive applications.

René P. A. Vugts received the B.Sc. and M.Sc. degrees in mechanical engineering from Eindhoven University of Technology, Eindhoven, The Netherlands, in November 2006 and January 2010, respectively. His M.Sc. study was focused on the string-stable cooperative adaptive cruise control design and experimental validation.

Since 2010, he has been a Visiting Scientist with the Control Systems Technology Group, Department of Mechanical Engineering, Eindhoven University of Technology.

Jeroen Ploeg was born in 1964. He received the M.Sc. degree in mechanical engineering from Delft University of Technology, Delft, The Netherlands, in 1988.

From 1989 to 1999, he was a Researcher with Koninklijke Hoogovens (currently Corus), Ijmuiden, The Netherlands, where his main interest was the dynamic process control of large-scale industrial plants. Since 1999, he has been a Senior Development Engineer with the Automotive Business Unit, Netherlands Organization for Applied Scientific Research. His current interests are focused on control system design for advanced driver-assistance systems and for path tracking of automatic guided vehicles. This work is executed in close cooperation with the Department of Mechanical Engineering, Eindhoven University of Technology, Eindhoven, The Netherlands, where he recently started his Ph.D. research on the synchronization of road vehicles for cooperative driving.

Marinus (René) J. G. van de Molengraft received the M.Sc. degree (*cum laude*) in mechanical engineering from Eindhoven University of Technology, Eindhoven, The Netherlands, in 1986 and the Ph.D. degree in 1990 on the identification of mechanical systems for control.

He is currently an Associate Professor with the Control Systems Technology Group, Department of Mechanical Engineering, Eindhoven University of Technology. He is an Associated Editor of *IFAC Mechatronics*. His current research interests include real-time control of embedded motion systems and the integrated design of intelligent mechatronic systems.

Maarten Steinbuch (S'83–M'89–SM'02) received the M.Sc. (*cum laude*) and Ph.D. degrees from the Delft University of Technology, Delft, The Netherlands, in 1984 and 1989, respectively.

From 1987 to 1999, he was with Philips Laboratories, Eindhoven. Since 1999, he has been a Full Professor and the Head of the Control Systems Technology Group, Department of Mechanical Engineering, Eindhoven University of Technology. Since July 2006, he has also been the Scientific Director of the 3TU Centre of Competence High-Tech Systems, Federation of Dutch Technical Universities. He is the Editor-in-Chief of *IFAC Mechatronics*. His research interests include the modeling, design, and control of motion systems and automotive powertrains.